0.1-μm Atomic Layer Deposition Al_2O_3 Passivated InAlN/GaN High Electron-Mobility Transistors for E-Band Power Amplifiers

Dong Xu, *Senior Member, IEEE*, K. K. Chu, J. A. Diaz, M. Ashman, J. J. Komiak, *Fellow, IEEE*,
L. Mt. Pleasant, C. Creamer, K. Nichols, K. H. G. Duh, P. M. Smith, *Fellow, IEEE*,
P. C. Chao, *Fellow, IEEE*, L. Dong, and Peide D. Ye, *Fellow, IEEE*

***Abstract*— High-performance 0.1-μm InAlN/GaN high electron-mobility transistors (HEMTs) have been successfully developed for power amplifiers operating at E-band (targeting 71–76 and 81–86-GHz bands). High maximum drain current of 1.75 A/mm and maximum extrinsic transconductance of 0.8 S/mm have been achieved for depletion-mode devices. Enhancement-mode HEMTs have also shown maximum drain current of 1.5 A/mm and maximum extrinsic transconductance of 1 S/mm. The selection of atomic layer deposition aluminum oxide (Al_2O_3) for device passivation enables a two-terminal breakdown voltage of ∼25 V, excellent subthreshold characteristics as well as the pulsed-*IV* featuring little current collapse for both types of HEMTs. When biased at a drain voltage of 10 V, a first-pass two-stage power amplifier design based on 0.1-μm depletion-mode devices has demonstrated an output power of 1.43 W with 12.7% power-added efficiency at 86 GHz, a level of performance that has been attained previously only by state-of-the-art counterparts based on AlGaN/GaN HEMTs at a much higher drain bias and compression level.**

***Index Terms*— HEMT, InAlN, GaN, ALD, millimeter-wave, power amplifier.**

I. INTRODUCTION

THE InAlN/GaN high electron-mobility transistor (HEMT) lattice matched to SiC substrate has generated a lot of interest in the past several years because of its excellent thermal stability, potential reliability advantage [1], and high sheet-carrier density. Several InAlN/GaN HEMTs have been reported, featuring excellent f_T for high-speed applications [2], [3]. Recently, interest also emerged in its potential for power applications at millimeter-wave (MMW) frequencies. This is primarily due to the much stronger spontaneous polarization of InAlN/GaN relative to AlGaN/GaN, which not only leads to a much higher drain current in the HEMT channel, but also allows the use of a much thinner InAlN gate layer, important for the shorter gate to limit short channel effects. However, it is interesting to note that the reports on power performance of InAlN/GaN HEMTs have been so far limited up to 30-40 GHz [4], [5], and monolithic microwave integrated circuits (MMIC's) for high-power applications at 71 GHz and beyond appear to be exclusively powered by AlGaN/GaN HEMTs [6]–[9]. We believe this reflects the increasingly challenging task to address the problem that the devices have to face to produce excellent large-signal performance at higher frequencies: pulsed-drain-current collapse due to trapping at the device surface, short channel effects related to inadequate aspect ratio, and a decrease in breakdown voltage partially resulting from the gate-length reduction.

In this letter, we report InAlN/GaN HEMTs tailored for MMIC power amplifiers (PA's) at E-band. A gate length of 0.1 μm has been selected to enable high operating frequency and to minimize short channel effects. Atomic layer deposition (ALD) aluminum oxide (Al_2O_3) is adopted as the passivation layer to alleviate trapping effects. In addition to depletion-mode (D-mode) HEMTs, enhancement-mode (E-mode) devices have also been fabricated to further explore vertical scaling and to evaluate the effectiveness of the ALD passivation. First-pass MMIC PA's based on D-mode devices have been fabricated as well, showing output power and power added efficiency (PAE) comparable to those only achieved so far by their state-of-the-art counterparts powered by AlGaN/GaN HEMTs.

II. DEVICE FABRICATION

The growth of epitaxial structures was performed with metalorganic chemical vapor deposition (MOCVD) on 4-inch semi-insulating SiC substrates. An undoped AlGaN buffer was adopted to serve as a back barrier to enhance the confinement of 2-dimentional electron gas in the channel. To achieve high aspect ratio and the resulting suppression of short channel effects, a nominally 1-nm undoped AlN layer, and a nominally 5-nm undoped InAlN gate layer with 17% indium were grown on top of a thin undoped GaN channel layer.

The fabrication process for 0.1-μm InAlN/GaN HEMTs includes inductively coupled plasma (ICP) mesa isolation etching, annealed Ge/Ti/Al/Ni/Au-based ohmic contact with 2-μm source-drain spacing, and the electron-beam lithography definition of 0.1-μm Γ-gates. Typical contact resistance is

Manuscript received February 11, 2015; accepted February 19, 2015. Date of publication March 5, 2015; date of current version April 22, 2015. The review of this letter was arranged by Editor S.-H. Ryu.

D. Xu, K. K. Chu, J. A. Diaz, M. Ashman, J. J. Komiak, L. Mt. Pleasant, C. Creamer, K. Nichols, K. H. G. Duh, P. M. Smith, and P. C. Chao are with Microelectronics Center, BAE Systems, Nashua, NH 03060 USA (e-mail: dong.xu@baesystems.com).

L. Dong and P. D. Ye are with the School of Electrical and Computer Engineering, Purdue University, West Lafayette, IN 47907 USA.

Digital Object Identifier 10.1109/LED.2015.2409264

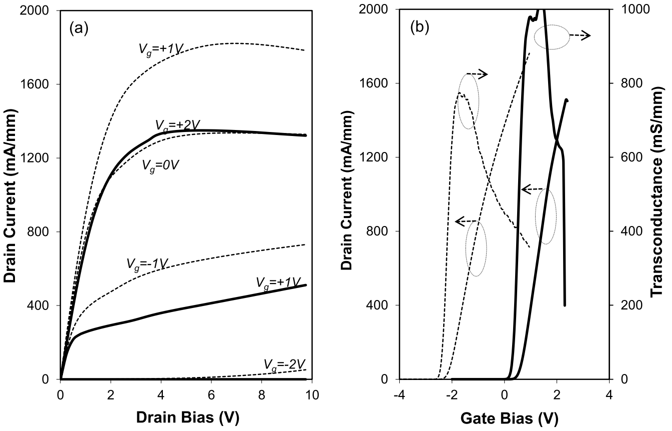

Fig. 1. Output *IV* characteristics (a) and transfer curves and transconductance (b) for 0.1-μm D- (dashed lines) and E-mode (solid lines) InAlN/GaN HEMTs with ALD Al_2O_3 passivation. The gate bias for the top curve of the *IV* characteristics is 1 and 2 V for D- and E-mode devices, respectively; the step of the gate bias is −1 V for both devices. The transfer curves and transconductances were measured at a V_{ds} of 10 V.

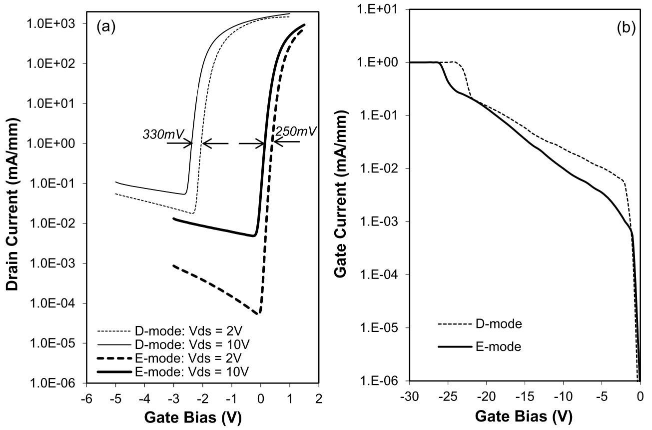

Fig. 2. (a) Transfer curves on a logarithmic scale for 0.1-μm D- (thin lines) and E-mode (thick lines) InAlN/GaN HEMTs with ALD Al_2O_3 passivation at a V_{ds} of 2 V (dashed lines) and 10 V (solid lines). (b) Reverse Schottky characteristics for 0.1-μm D- (dashed line) and E-mode (solid line) InAlN/GaN HEMTs with ALD Al_2O_3 passivation.

about 0.2 Ω-mm. In addition to regular D-mode devices, E-mode HEMTs have also been fabricated on the same wafer with about 3-nm recess etching using BCl_3 plasma before the gate metallization onto the InAlN layer as D-mode devices. To effectively alleviate trapping effects, ALD Al_2O_3 has been selected as the passivation layer due to the outstanding quality of its interface with the InAlN gate layer. A 3-nm ALD Al_2O_3 layer was grown with an ASM F-120 ALD system, and details of the deposition process can be found in [10]. Typically, the sheet resistance of the wafer is 305 Ω/sq after growth at room temperature; it drops to about 250 Ω/sq after passivation. In addition, a plasma enhanced chemical vapor deposition (PECVD) SiN was also introduced at later stage of the fabrication as the second passivation layer. The SiC substrate was thinned to 55 μm to enable the fabrication of 15 μm × 25 μm slot via holes, important for realizing low inductance and highly compact devices to facilitate MMW MMIC design [11].

III. RESULTS AND DISCUSSION

Fig. 1(a) and Fig. 1(b) are the *IV* and transfer characteristics of the D- (dashed lines) and E-mode HEMTs (solid lines) with ALD Al_2O_3 passivation. The D-mode device shows a drain current of about 1.75 A/mm at a gate bias V_{gs} of 1 V and a drain bias V_{ds} of 10 V, higher than that of the E-mode device because of the shift in pinch-off voltage V_{po}. However, the E-mode device can still attain a drain current of 1.5 A/mm if biased at $V_{gs} = 2.4$ V and $V_{ds} = 10$ V, when a gate current of 10 mA/mm is reached. The on-resistances for the D- and E-mode devices are about 1.1 (at $V_{gs} = 1$ V) and 1.3 Ω-mm (at $V_{gs} = 2.4$ V), respectively, even with their relatively large source-drain spacing of 2 μm. The D- and the E-mode devices show V_{po} of about −2.42 and 0.23 V respectively; their corresponding standard deviations are 40 and 70 mV, with the latter also indicating good uniformity of the gate recess for the E-mode devices. In addition to the sharp pinch-off, maximum extrinsic transconductances as high as 0.8 and 1 S/mm have been achieved for the D- and E-mode devices, respectively, at a V_{ds} of 10 V. This is due primarily to their high intrinsic transconductances of 1.1 and 1.6 S/mm arising from epitaxial design and the gate recess for E-mode FETs.

Further evidence of excellent device scaling can be found in Fig. 2(a), which shows the transfer curves of the D- (thin lines) and E-mode devices (thick lines) at a V_{ds} of 2 (dashed lines) and 10 V (solid lines) plotted on a semi-logarithmic scale. The D- and E-mode devices display not only a small V_{po} shift of about 330 and 250 mV when V_{ds} is increased from 2 to 10 V, but also a low subthreshold swing (SS) of 112 and 81 mV/decade at $V_{ds} = 2$ V and 122 and 108 mV/decade at $V_{ds} = 10$ V, respectively. The low reverse gate current as shown in Fig. 2(b) is also partially attributed to the high aspect ratio of devices. The 25 and 27 V gate-drain breakdown voltages for the D- and E-mode devices are sufficient for operation at $V_{ds} = 10$ V.

The pulsed-*IV* characterization was performed with a pulse width of 200 ns and a separation of 2 ms. Fig. 3(a) shows that the D-mode device has a drain current collapse of about 50 mA/mm at $V_{ds} = 5$ V and 100 mA/mm at $V_{ds} = 2.5$ V, when the quiescent point is switched from $V_{gs} = 0$ V and $V_{ds} = 0$ V to $V_{gs} = -5$ V and $V_{ds} = 10$ V. As expected, the E-mode device suffers more current collapse as shown in Figure 3(b). However, the ALD passivation has contained its collapse to 50 mA/mm at $V_{ds} = 5$ V and 140 mA/mm at $V_{ds} = 2.5$ V.

Fig. 3(c) compares the dc (dotted lines) and pulsed drain current (dashed and solid lines) of the D-mode devices that are passivated by the Al_2O_3 layers (thick lines) and the PECVD SiN (thin lines) with comparable thickness. The ALD device shows about 3% higher dc maximum drain current than its SiN counterpart at a low V_{ds} of 3 V. The performance advantage brought by the Al_2O_3 passivation becomes even more obvious when the pulsed drain current is recorded. The Al_2O_3 device has about 10% and 12% higher pulsed maximum drain current than that of the SiN device

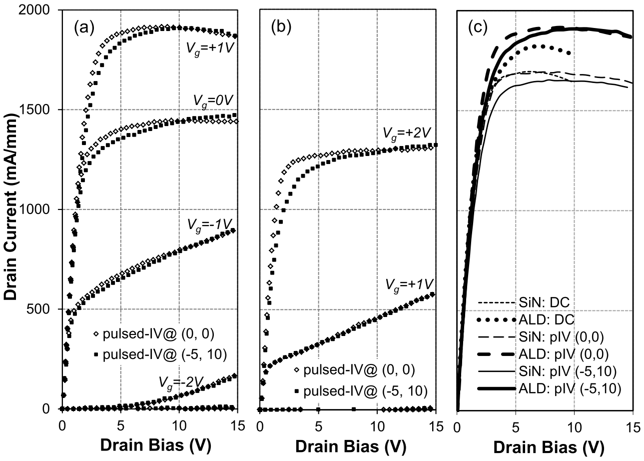

Fig. 3. Pulsed-*IV* characteristics for 0.1-μm (a) D- and (b) E-mode InAlN/GaN HEMTs with ALD Al_2O_3 passivation. The devices were measured at quiescent points of $V_{gs} = 0$ V and $V_{ds} = 0$ V (open symbols) and $V_{gs} = -5$ V and $V_{ds} = 10$ V (solid symbols). The V_{gs} for the top curves is 1 and 2 V for D- and E-mode devices, respectively, and the V_{gs} step is -1 V for both devices. (c) Comparison between dc and pulsed drain current for 0.1-μm D-mode devices with PECVD SiN (thin lines) and ALD Al_2O_3 (thick lines) passivation. Each curve in (c) was measured at a V_{gs} of 1 V.

TABLE I

SUMMARY OF REPORTED MILLIMETER-WAVE MMIC PA'S AT 75 GHz OR HIGHER [6]–[9] AND THE E-BAND MMIC PA BASED ON THE 0.1-μm D-MODE InAlN/GaN HEMTs IN THIS WORK; THE LATTER WAS MEASURED AT $V_{ds} = 10$ V AND $I_{ds} = 500$ mA/mm. THE RESULT FROM [8] WAS OPTIMIZED FOR HIGH OUTPUT POWER

Ref.	HEMT	# Stages	Freq (GHz)	V_{ds} (V)	Gain Comp (dB)	P_{out} (W)	PAE (%)	Power Gain (dB)
[6]	0.12μm AlGaN	3	75	35	5	1.3	6	6
[7]	0.15μm AlGaN	3	88	14	5	0.84	14.7	9.3
[8]	0.15μm AlGaN	3	91	20	3	1.7	11	12
[9]	0.14μm AlGaN regrown ohmic	3	93.5	14	5	2.14	19	11
This work	0.1μm InAlN w/ ALD Al_2O_3	2	86	10	1.5	1.43	12.7	8.5

at quiescent point of $V_{gs} = 0$ V and $V_{ds} = 0$ V and at the deep pinch-off bias of $V_{gs} = -5$ V and $V_{ds} = 10$ V, respectively. The higher pulsed drain currents of the ALD device result from its on-resistances that are 16% lower than the SiN device as indicated in the pulsed-*IV* in Fig. 3(c), showing the effectiveness of ALD passivation.

On-wafer s-parameter measurement was performed over 0.5-110 GHz at a V_{ds} of 10 V and drain current of 500 mA/mm. The 2 × 35 μm D-mode HEMT showed an estimated current gain cut-off frequency f_T of 100 GHz (identical to E-mode) and a maximum available gain (MAG) of about 7 dB at 86 GHz. A 2-stage E-band MMIC PA has been designed based on the 0.1-μm D-mode HEMT, demonstrating an output power of 1.43 W and associated PAE of 12.7% at a 1.5-dB compression (where the amplifier is not being driven fully into compression due to limitations of the test setup). As summarized in Table 1, this result, while being limited in compression level by input drive, is better than the 1.3 W and 6% at 75 GHz in [6], comparable to the 0.84 W and 14.7% at 88 GHz in [7], as well as the 1.7 W and 11% at 91 GHz in [8]; it has lower output power and PAE than that reported in [9]. It should be noted, however, the InAlN/GaN material system allows further improvement in device vertical scaling due to its higher sheet charge achievable with thinner barrier layers in comparison with AlGaN barrier devices. As a result, shorter gate lengths can be used in InAlN/GaN power devices while maintaining proper aspect ratio. With continued device optimization including lateral scaling like that in [9], InAlN/GaN HEMT technology can pave the way for further MMIC PA improvement at E-band and beyond.

IV. CONCLUSION

0.1-μm D- and E-mode InAlN/GaN HEMTs have exhibited excellent dc characteristics including maximum drain current of 1.75 and 1.5 A/mm, maximum extrinsic transconductance of 0.8 and 1 S/mm, and two-terminal breakdown of about 25 and 27 V, respectively. The ALD Al_2O_3 passivated devices have also showed excellent sub-threshold characteristics and 10-12% higher pulsed drain current over those passivated with PECVD SiN. The 0.1-μm D-mode InAlN/GaN HEMT enables the demonstration of a 2-stage MMIC PA achieving a 1.43 W output power and 12.7% associated PAE at 86 GHz, clearly showing its promise for power amplifiers in this MMW range.

ACKNOWLEDGMENT

The authors would like to thank R. Carnevale and R. Isaak for layout, P. Seekell, A. Vera, J. Pare, L. Schlesinger, S. Brun, M. Gerlach, D. Gallagher, J. Hulse, J. Kanjia, W. H. Zhu, K. Tourigny and X. P. Yang for processing assistance, J. Lombardi and F. Ducharme for testing, and A. K. Stewart, S. Sweetland, and S. Powell for the program support.

REFERENCES

[1] E. Kohn *et al.*, "InAlN HEMTs: Design-technology-performance," in *Extended Abstract Lester Eastman Biennial Conf. High Perform. Devices*, Newark, DE, USA, Aug. 2008.
[2] D. S. Lee *et al.*, "300-GHz InAlN/GaN HEMTs with InGaN back barrier," *IEEE Electron Device Lett.*, vol. 32, no. 11, pp. 1525–1527, Nov. 2011.
[3] M. L. Schuette *et al.*, "Gate-recessed integrated E/D GaN HEMT technology with $f_T/f_{max} > 300$ GHz," *IEEE Electron Device Lett.*, vol. 34, no. 6, pp. 741–743, Jun. 2013.
[4] A. Crespo *et al.*, "High-power Ka-band performance of AlInN/GaN HEMT with 9.8-nm-thin barrier," *IEEE Electron Device Lett.*, vol. 31, no. 1, pp. 2–4, Jan. 2010.
[5] S. Tirelli *et al.*, "AlInN-based HEMTs for large-signal operation at 40 GHz," *IEEE Trans. Electron Devices*, vol. 60, no. 10, pp. 3091–3098, Oct. 2013.
[6] Y. Nakasha *et al.*, "E-band 85-mW oscillator and 1.3-W amplifier ICs using 0.12 μm GaN HEMTs for millimeter-wave transceivers," in *Proc. IEEE Compound Semiconductor Integr. Circuit Symp.*, Monterey, CA, USA, Oct. 2010, pp. 1–4.
[7] M. Micovic *et al.*, "W-band GaN MMIC with 842 mW output power at 88 GHz," in *IEEE MTT-S Int. Microw. Symp. Dig.*, Anaheim, CA, USA, May 2010, pp. 237–239.
[8] A. Brown *et al.*, "W-band GaN power amplifier MMICs," in *IEEE MTT-S Int. Microw. Symp. Dig.*, Baltimore, MD, USA, Jun. 2011, pp. 1–4.
[9] M. Micovic *et al.*, "92–96 GHz GaN power amplifiers," in *IEEE MTT-S Int. Microw. Symp. Dig.*, Montreal, QC, Canada, Jun. 2012, pp. 1–3.
[10] D. Xu *et al.*, "0.2-μm AlGaN/GaN high electron-mobility transistors with atomic layer deposition Al_2O_3 passivation," *IEEE Electron Device Lett.*, vol. 34, no. 6, pp. 744–746, Jun. 2013.
[11] D. Xu *et al.*, "Advanced no-field-plate AlGaN/GaN HEMTs for millimeter-wave MMIC applications," in *Proc. Lester Eastman Biennial Conf. High Perform. Devices*, Ithaca, NY, USA, Aug. 2014, pp. 1–3.